

¹ Context-dependent consequences of lagged effects in
² demographic models

³ Eric R. Scott¹, María Uriarte¹, Emilio M. Bruna¹

⁴ ¹Department of Wildlife Ecology and Conservation, University of Florida, Gainesville,
⁵ Florida 32611-0430 USA

⁶ ²Department of Ecology, Evolution and Environmental Biology, Columbia University 1200
⁷ Amsterdam Avenue, New York, New York 10027 USA

⁸ ³Center for Latin American Studies, University of Florida, Gainesville, Florida 32611-5530
⁹ USA

¹⁰ ⁴Biological Dynamics of Forest Fragments Project, INPA-PDBFF, CP 478, Manaus,
¹¹ Amazonas 69011-970 Brazil

¹² (draft: 8 September 2025)

¹³

Abstract

¹⁴ Text of 150 words max summarizing this amazing paper.

¹⁵ **Keywords:** demography, environmental stochasticity, integral projection models,

¹⁶ lagged effects, structured population models, population dynamics

¹⁷ **Manuscript elements:** Figures 1-4, Tables 1-6

¹⁸ **Manuscript type:** e-note

19

Introduction

20 Current environmental conditions can have large and immediate effects on the growth,
21 survival, or reproduction of long-lived organisms. There is also mounting evidence, however,
22 for intervals that range from months to years between environmental conditions and the
23 resulting changes in demographic vital rates. These *Lagged Effects*, also known as *Delayed*
24 *Life-history Events* (i.e., DLHEs) (Beckerman et al. 2002), can simultaneously affect an
25 entire cohort (e.g., juveniles hatching during a period of scarcity will all have delayed
26 maturation and lower lifetime fecundity) or only a subset of the population (e.g., cold
27 temperatures in one year lead to reduced flowering by potentially reproductive individuals
28 in the next). In addition, the temporal delay between an environmental event and changes
29 in demographic vital rates depends on both the intensity of the event and its timing
30 relative to the underlying physiological processes (Criley and Lekawatana 1994; Evers et al.
31 2021). A drought during the early stages of gestation or floral bud formation, for example,
32 might have a much larger impact on the number of fruits or offspring produced than one at
33 a later stage of the reproductive process. The delay or intensity of lagged effects can also
34 be location- or habitat-specific, with individuals in some sites or habitats buffered against,
35 or able to recover more quickly from, the delayed effects of environmental variation.

36 Because Lagged Effects are often directly linked to reproduction and survival, it has
37 been argued they could have major but underappreciated consequences for population
38 dynamics (Beckerman et al. 2002). While recent studies suggest this could indeed the case
39 (Williams et al. 2015; e.g., Molowny-Horas et al. 2017; Tenhumberg et al. 2018), broader
40 efforts to test this hypothesis have face a number of obstacles (Metcalf et al. 2015).

41 Empirical tests of putative lagged effects are rare because these are challenging to design,
42 implement, and maintain (Kuss et al. 2008). While one could conceivably use
43 observational data to detect lagged effects, doing so requires long-term data on both the
44 putative lagged effect (e.g., reduced probability of flowering) and its potential

45 environmental drivers (e.g., drought during early floral development), and such coupled
46 data sets are rare (*sensu* Evers et al. 2021). In addition, the methods for both identifying
47 lagged effects and modeling their demographic impacts can be challenging to implement.
48 For example, many of the potentially applicable statistical methods have stringent
49 assumptions and data requirements rarely met by ecological data (Metcalf et al. 2015),
50 while the including complex biological processes in demographic models can render them
51 less tractable or amenable to analysis using currently available tools. Addressing these
52 challenges is a major undertaking; the value of doing so will depend on the effort required
53 vs. the potential consequences of failing to consider lagged effects — consequences that
54 range from overestimating projections of population growth rate (i.e., λ) in a conservation
55 setting to drawing invalid conclusions regarding support for the predictions of ecological or
56 evolutionary theory.

57 Integral Projection Models (i.e., IPMs) are an important and widely used tool for
58 studying demography and population dynamics (Ellner and Rees 2006; Rees and Ellner
59 2009; Rees et al. 2014). Their flexibility, in concert with a rapidly growing suite of
60 software, data, and other resources (Salguero-Gómez et al. 2015; Ellner et al. 2016; Levin
61 et al. 2021), have facilitated their use to study a wide range of topics in ecology, evolution,
62 and conservation (Morris and Doak 2002; Crone et al. 2011; Ellner et al. 2016).
63 Mathematical and statistical advances (e.g., Williams et al. 2012; Brooks et al. 2019) have
64 rapidly expanded the scope of questions and biological processes that can be investigated
65 with these models (e.g., Metcalf et al. 2015; Ellner et al. 2016; Rees and Ellner 2016). Here
66 we investigate how including lagged effects in Integral Projection Models influences
67 projections of λ and population structure.

68 We have previously shown that the effects of precipitation extremes on the
69 demographic vital rates of an Amazonian understory herb (*Heliconia acuminata*,
70 Heliconiaceae) can be delayed up to 36 months (Scott et al. 2022), with the presence and
71 duration of these lagged effects varying by vital rate and habitat. We parameterized three

72 classes of Integral Projection Models — a deterministic IPM, a stochastic IPM, and a
73 stochastic IPM with lagged effects of precipitation on vital rates — for populations in two
74 habitat types (i.e., continuous forest vs. forest fragments). Based on previous studies
75 (Bruna and Kress 2002; Bruna 2003; Bruna and Oli 2005) and demographic theory
76 (Tuljapurkar 1990; Caswell 2001) we predicted that: (i) projections of λ from deterministic
77 models would be higher than those of stochastic models, and that (ii) λ is lower for Forest
78 Fragment than Continuous Forest populations regardless of model, but the difference
79 between the two habitats is greatest for the IPM with lagged effects.

80 **Methods**

81 ***Study System and Demographic Data***

82 *Heliconia acuminata* (Heliconiaceae) is a perennial, self-incompatible monocot that is
83 distributed throughout much of the Amazon basin (Kress 1990). While some *Heliconia*
84 species grow in large aggregations on roadsides, gaps, and in other disturbed habitats,
85 others, including *H. acuminata*, grow primarily in the forest understory (Kress 1983;
86 Ribeiro et al. 2010). Understory *Heliconia* species produce fewer flowers and are pollinated
87 by traplining hummingbirds (Stouffer and Bierregaard 1996; Bruna et al. 2004). The
88 models and analyses here are based on 11 years (1998-2009) of demographic data collected
89 on >8500 *H. acuminata* found at Brazil's Biological Dynamics of Forest Fragments Project
90 (BDFFP), located ~70 km north of Manaus, Brazil. The BDFFP reserves include both
91 continuous forest and forest fragments that range in size from 1-100 ha. These fragment
92 reserves were originally isolated in the early 1980's by the creation of cattle pastures, with
93 the secondary growth surrounding them periodically cleared to ensure their continued
94 isolation. The habitat in all sites is non-flooded lowland rain forest with rugged
95 topography. A complete summary of the BDFFP and its history can be found in
96 Bierregaard et al. (2001).

97 A complete description of our demographic methods, data, and analyses to date can be
98 found in Bruna et al. (2023). Briefly, in 1997–1998 a series of 5000 m² plots were
99 established in the BDFFP reserves: N=6 in Continuous Forest and N=4 in 1-ha Forest
100 Fragments (i.e., CF and FF, respectively). All of the *Heliconia acuminata* in these plots
101 were marked and measured; the plots were censused annually, at which time a team
102 recorded the size of surviving individuals, marked and measured new seedlings, and
103 identified any previously marked plants that died. Each plot was also surveyed 4-5 times
104 during the flowering season to identify reproductive plants. These surveys were
105 complemented by data on the number of fruits per flowering plant (Bruna 2021) and seeds
106 per fruit (Bruna 2014) that were collected outside of the demographic plots to avoid
107 altering within-plot recruitment. We also conducted experiments to quantify the
108 probability of seed germination and seedling establishment in both forest fragments and
109 continuous forest (Bruna 1999, 2002).

110 The rainy season in our sites is typically from late December through late May.
111 *Heliconia acuminata* in our site begin flowering early in the rainy season and most
112 reproductive plants produce a single inflorescence (range = 1–7) with 20–25 flowers (Bruna
113 and Kress 2002). Fruits mature April-May and have 1–3 seeds per fruit ($\bar{x} = 2$) that are
114 dispersed by a thrush and several species of manakin (Uriarte et al. 2011). Dispersed seeds
115 germinate approximately 6 months after dispersal at the onset of the subsequent rainy
116 season, with rates of germination and seedling establishment higher in continuous forest
117 than forest fragments (Bruna 1999, 2002). On average, plots in CF also had more than
118 twice as many plants as the plots in 1-ha fragments (CF median = 788, range =
119 (201-1549); 1-ha median = 339, range = (297-400)).

120 ***Construction of Integral Projection Models***

121 We projected the growth rate and structure of *Heliconia acuminata* with three classes of
122 IPMs: Deterministic, Stochastic, and Stochastic with Lagged Environmental Effects. Each

123 of these IPMs required different functional forms of the underlying vital rate functions used
 124 to describe the *H. acuminata* life cycle (Figure 1). All models were density-independent,
 125 with the deterministic model serving as the foundation for the more complex models. Our
 126 modeling workflows were managed using the `targets` R package (Landau 2021); in
 127 addition to ensuring reproducibility this allowed us to track computational time spent
 128 processing and analyzing each class of IPM.

129 **(1) Deterministic IPM:** In this model the size and structure of a population in year
 130 $t + 1$ is determined by the survival and growth of plants alive in year t (Equation 1) plus
 131 the number of new seedlings that entered the population (Equation 2).

$$n(z', t + 1) = R(z')n_s(t) + \int_L^U P(z', z)n(z, t) dz \quad (1)$$

$$n_s(t + 1) = \int_L^U F(z)n(z, t) dz \quad (2)$$

132 Equation 1 has two components. The first is the sub-kernel $P(z', z)$, which describes
 133 the size-dependent survival and growth/regression of mature plants (Equation 3):

$$P(z', z) = s(z)G(z', z) \quad (3)$$

134 The second is sub-kernel $R(z')$, which describes the survival of seedlings established in
 135 year t and their size when entering the mature plant population in year $t + 1$ (Equation 4):

$$R(z') = s_s G_s(z') \quad (4)$$

136 Note that in Equation 4 both the probability that new seedlings survive their first year,
 137 s_s , and their size at the end of this year, $G(z', z)$, are size-independent. IPMs can include
 138 transitions between individuals from a discrete state to a continuous one (i.e., from
 139 ‘seedling’ to ‘mature plant of size z' ,’ Ellner et al. 2016); we treat seedlings as a distinct

¹⁴⁰ and discrete category because they have lower survival and growth in their first year than
¹⁴¹ comparably sized plants (Bruna 2003; Scott et al. 2022).

¹⁴² The number of new seedlings entering the population in year $t + 1$ is a function of the
¹⁴³ number of mature plants in year t and a sub-kernel describing the size-dependent fecundity
¹⁴⁴ of these individuals (Equation 5):

$$F(z) = p_f(z)f(z)g \quad (5)$$

¹⁴⁵ Both the probability that a mature plant will flower, $p_f(z)$, and the number of seeds a
¹⁴⁶ flowering plant will produce, $f(z)$, are size-dependent. All seeds germinate and establish as
¹⁴⁷ seedlings with probability g .

¹⁴⁸ We used the annual census data (Bruna 2003) to fit the deterministic vital rate
¹⁴⁹ functions for growth, survival, and flowering in each habitat type (i.e., Fragments,
¹⁵⁰ Continuous Forest; the data from all plots within a habitat class were pooled to create a
¹⁵¹ single ‘summary population’ for the CF and FF habitats (Bruna 2003). For established
¹⁵² plants these were modeled as a smooth function of size in the previous census with
¹⁵³ generalized additive models (GAMs) fit with the `mgcv` package (Wood 2011) for the R
¹⁵⁴ statistical programming language (R Core Team 2020). For consistency, seedling survival
¹⁵⁵ and growth were also modeled using GAMs, but without size in the previous census as a
¹⁵⁶ predictor (i.e. ‘intercept-only’ models). For growth models a scaled t family distribution
¹⁵⁷ provided a better fit to the data than a Gaussian fit, as the residuals with a simple
¹⁵⁸ Gaussian model were Leptokurtic. To model size-specific fecundity we used the data on
¹⁵⁹ fruits per flowering plant (Bruna 2021), seeds per fruit (Bruna 2014), and the
¹⁶⁰ experimentally-derived estimates of seed germination and seedling establishment (Bruna
¹⁶¹ 1999, 2002).

¹⁶² **(2) Stochastic IPMs:** To include temporal stochasticity in our IPMs we included a
¹⁶³ random effect of year. This was done using a factor-smooth interaction that allowed the

164 functional form of the relationship between plant size and vital rates to vary among
165 transition years (Figure 1). We generated kernels for every transition year using the
166 long-term survey data (Bruna et al. 2023) and random smooths for year. We then
167 randomly selected one of these sets of kernels to use in each iteration of the IPM. This
168 procedure is equivalent to ‘*kernel resampling*’ (*sensu* Metcalf et al. 2015) or matrix
169 selection for matrix population models (Caswell 2001).

170 **(3) Stochastic IPMs with lagged effects of precipitation on vital rates:** We
171 explicit modeled the lagged effects of precipitation extremes on vital rates using the
172 procedure described in Scott et al. (2022). Briefly, we first calculated the Standardized
173 Precipitation Evapotranspiraton Index (i.e., SPEI) for our study site using a published
174 gridded dataset based on ground measurements (Xavier et al. 2016). After we fit vital rate
175 models using the long-term survey data (Figure 1), we modeled delayed effects of SPEI
176 with Distributed Lag Non-linear Models (i.e., DLNMs) with a maximum lag of 36 months
177 (Scott et al. 2022). To iterate these parameter-resampled IPMs (*sensu* Metcalf et al. 2015)
178 we first created a random sequence of SPEI values by sampling years of the observed
179 (monthly) SPEI data. For every year we then calculated a lag of 36 months from the
180 month in which that year’s census was completed. These values were then used to predict
181 the fitted values from vital rate models, which generated different kernels for each iteration
182 of the IPM. The kernels of successive iterations are not entirely independent — the SPEI
183 values used to calculate vital rates include values used in the previous two iterations — but
184 they are ergodic.

185 All IPMs were constructed and iterated using the `ipmr` package (Levin et al. 2021) for
186 the R statistical programming language (R Core Team 2020). The IPMs used 100
187 meshpoints and the midpoint rule for calculating kernels. For each type of IPM we iterated
188 the model for 1000 time steps, but discarded the first 100 time steps to omit transient
189 effects. Stochastic growth rates (λ_s) were calculated as the average $\ln(\lambda)$ from each time
190 step (Caswell 2001) and then back-transformed to allow for direct comparison with

projections of λ from deterministic models. The initial starting vector primarily influences a population's transient dynamics; we therefore used the distribution of established plant sizes and proportion of seedlings in the full demographic data set as the initial population vector for all models.

Finally, We estimated the 95% confidence intervals for each IPMs projections of λ . To do so we first created 500 populations for each habitat type by sampling individual plants with replacement (i.e., bootstrapping) until the population size of each matched that of the initial population vector. We then re-fit the vital rate models for growth, survival, and flowering for each of these bootstrapped population and constructed new IPMs for each population as above (the models for germination and establishment rate, fruits per flowering plant, and seeds per fruit were not refit because these were estimated using different data sets). The projections of λ for the new populations were then used to estimate the upper and lower 95% bias-corrected percentile intervals (Caswell 2001; Manly 2018).

205 *Statistical analyses*

206 **Comparison of λ in Continuous Forest and Forest Fragments.** To determine if the deterministic projections of λ for Continuous Forest and Forest Fragment populations were significantly different we used the randomization test procedure described by Caswell (2001). Briefly, we randomly assigned plants with their demographic history among two populations, R_1 and R_2 , that were equal in size to the original CF and FF populations. We then calculated λ^{R_1} , λ^{R_2} , and the absolute value of the difference between the two (i.e., θ). This was repeated $N = 1000$ times, after which we determined the proportion of simulations in which θ was greater than the observed difference between λ^{CF} and λ^{FF} (i.e., $P[\theta \geq \theta_{obs}]$).

215 We used a Generalized Linear Model to compare the projections of λ from the two stochastic IPMs. We modelled the lambda as a function of IPM type (kernel-resampling vs

parameter-resampling) and Habitat (continuous forest vs. fragments), and the interaction of IPM type and Habitat. Because the response variable (λ) was continuous we used the Gaussian distribution with the identity link function in our model. We verified the model assumptions by plotting residuals versus fitted values.

Population Structure. Finally, we compared the structure of populations through the first 250 time steps in each habitat by each of the stochastic IPMs (i.e, kernel- vs. parameter-resampling). At each time step, we assigned the individuals to one of four stage classes based on plant size, probability of survival, and probability of reproduction (see Table Table 3). We then calculated the proportion of the population that was in each stage class in each habitat for each IPM type. Comparing the means and variances of these proportions will allow us to determine (1) if the two IPMs project different population structures over time, (2) if the population structure for a given IPM is consistent across habitat type. Because Shapiro-Wilk tests indicated that the distributions of proportions were not normally distributed, we used the non-parametric Ansari-Bradley Test to compare the distribution of proportions in each habitat x stage combination. These analyses were conducted using the R packages `rstatix` and `vartest`, respectively (Kassambara 2023; Cosar and Dag 2024).

Results & Discussion

All IPMs projected higher population growth rates for *Heliconia acuminata* populations in Continuous Forest than for those in Forest Fragments (Table 2, Table 6). The differences between λ^{CF} and λ^{FF} , which ranged from 1.19-2%, were significant for both deterministic ($P[\theta \geq \theta_{obs}] = 0$, $N = 1000$ randomization) and stochastic IPMs (Table 6). There were also significant effects of IPM Type, Habitat, and their interaction on λ (Table 6). Because stochasticity is predicted to reduce population growth rates (Tuljapurkar et al. 2003; Doak et al. 2005; Metcalf et al. 2015), we were surprised to find that deterministic λ was nearly

242 identical to the average λ from kernel-resampled IPMs (Figure 3). However, we did see
243 reductions in population growth rate when including lagged effects in IPMs: on average the
244 projections of λ from these models were 1.5-2% lower, with 70-76% of the values below
245 deterministic λ (Figure 3). The IPMs with lagged effects also appear to be more accurate
246 — the underlying vital rate models for IPMs with lagged effects all had the best fit to the
247 survey data ($dAIC = 0$, Table 1).

248 Including lagged effects in IPMs also resulted in significantly less predictable
249 projections of population structure, both within (Figure 2 a) and across habitats (Figure 2
250 b, Table 4). This variability is particularly notable in forest fragments (Figure 4, Table 5),
251 where we have previously shown lagged effects have very large impacts on growth and
252 survival (Scott et al. 2022). The deterministic IPM for Continuous Forest projected
253 slightly more of the smallest and largest plants than the one for Forest Fragments. In other
254 words, populations in forest fragments had proportionately less recruitment and fewer
255 individuals growing into the larger, reproductive size classes (Bruna and Oli 2005). This
256 shift towards intermediately sized, pre-reproductive plants in forest fragments is even more
257 dramatic when using the parameter-resampled stochastic IPM (Figure 2 b).

258 What are the implications of these results for the use of IPMs to study plant
259 demography? First, they suggest that failing to include lagged effects in models could
260 significantly underestimate the growth rate of populations. While relative differences in
261 projections of λ may be sufficient for some tests of theory, the actual value of projections
262 may be critical in conservation or management settings. For example, they could be used to
263 identify which populations face the greatest risk of extinction (e.g., $\lambda = 0.99$ vs. $\lambda = 1.01$)
264 or — because even small differences in λ can have major short-term consequences for
265 population dynamics (e.g., $\lambda = 1.01$ vs. $\lambda = 1.02$) — be used to choose among management
266 strategies. Moreover, including lagged effects in models could be especially critical for
267 studies assessing the effects of climate change, given many DLHE are climate driven. That
268 said, there is a cost to including lagged effects in demographic models, even when doing so

269 is conceptually appropriate or if the outcome is potentially more accurate. While
270 Deterministic and Kernel-resampled Stochastic IPMs took only ~0.02 and ~0.07 min to
271 iterate (respectively), the Stochastic IPMs with using parameter-resampled kernels and
272 lagged effects took ~87.12 min. This is largely due to the required computational resources
273 and algorithms (i.e., `predict()`), which are much slower for Generalized Additive Models
274 with 2D smooths because of the much higher number of knots than for the GAMs used in
275 Deterministic and Kernel-resampled IPMs. Advances in computational power and access to
276 high-performance computing resources could lower this cost.

277 That said, computational power cannot compensate for limited data. Detecting lagged
278 effects and evaluating their consequences requires long-term demographic data — data that
279 are only available for a relatively small number of species, few of which are in the tropics.
280 The increasing evidence that lagged effects are ubiquitous, and that they can have major
281 demographic impacts, underscores the need to support the collection of such long-term
282 data, the complementary development of experimental and statistical approaches to
283 disentangling lagged effects, and community driven efforts to identify priority or model
284 systems for in-depth investigation.

285 Acknowledgments

286 We thank _____, _____, and _____ anonymous reviewers for helpful discussions and
287 comments on the manuscript. We also thank Sam Levin for his help with the `ipmr` package.
288 Financial support for collecting the demographic data used in this study was provided by
289 the U.S. National Science Foundation (awards INT 98-06351, DEB-0309819,
290 DEB-0614149, DEB-0614339, and DEB-1948607). This article is publication no. _____ in
291 the BDFFP Technical series. The authors declare no conflicts of interest.

292

CRediT Statement

293 ERS contributed to the conceptualization, methodology, formal analysis, and led the
294 writing of the original draft. EMB contributed to the conceptualization, methodology,
295 writing, and, acquired funding.

296

Data Availability Statement

297 Data and R code used in this study are archived with Zenodo at (*doi and url to be added*
298 *on acceptance*).

Literature Cited

- 300 Beckerman, A., T. G. Benton, E. Ranta, V. Kaitala, and P. Lundberg. 2002. Population
301 dynamic consequences of delayed life-history effects. Trends in Ecology & Evolution
302 17:263–269.
- 303 Bierregaard, R. O., C. Gascon, T. E. Lovejoy, and R. Mesquita, eds. 2001. Lessons from
304 Amazonia: The ecology and conservation of a fragmented forest. Yale University Press,
305 New Haven.
- 306 Brooks, M. E., K. Kristensen, M. R. Darrigo, P. Rubim, M. Uriarte, E. Bruna, and B. M.
307 Bolker. 2019. Statistical modeling of patterns in annual reproductive rates. Ecology 100.
- 308 Bruna, E. M. 1999. Seed germination in rainforest fragments. Nature 402:139.
- 309 ———. 2002. Effects of forest fragmentation on *Heliconia Acuminata* seedling recruitment
310 in central Amazonia. Oecologia 132:235–243.
- 311 Bruna, E. M. 2003. Are plant populations in fragmented habitats recruitment limited?
312 Tests with an Amazonian herb. Ecology 84:932–947.
- 313 ———. 2014. Dataset: *Heliconia Acuminata* seed set (seeds per fruit). Figshare doi:
314 10.6084/m9.figshare.1273926.v2.
- 315 ———. 2021. Dataset: Leaf number, leaf area, shoot number, and height of reproductive
316 *H. Acuminata*. Zenodo <https://doi.org/10.5281/zenodo.5041931>.

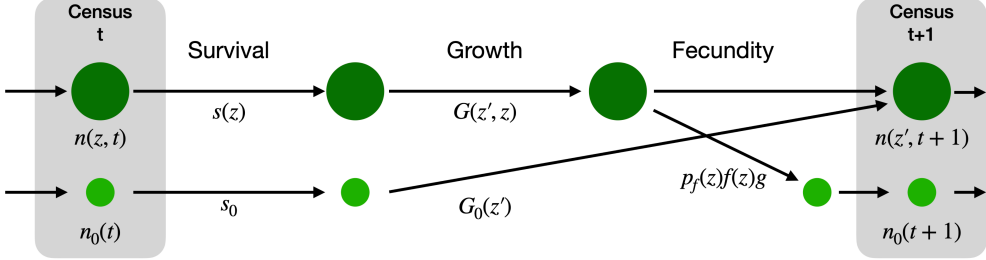
- ³¹⁷ Bruna, E. M., and W. J. Kress. 2002. [Habitat fragmentation and the demographic structure of an Amazonian understory herb \(*Heliconia Acuminata*\)](#). Conservation Biology 16:1256–1266.
- ³²⁰ Bruna, E. M., W. J. Kress, F. Marques, and O. F. da Silva. 2004. [*Heliconia Acuminata* reproductive success is independent of local floral density](#). Acta Amazonica 34:467–471.
- ³²² Bruna, E. M., and M. K. Oli. 2005. [Demographic Effects of Habitat Fragmentation on a Tropical Herb: Life-Table Response Experiments](#). Ecology 86:1816–1824.
- ³²⁴ Bruna, E. M., M. Uriarte, M. R. Darrigo, P. Rubim, C. F. Jurinitz, E. R. Scott, O. Ferreira da Silva, et al. 2023. [Demography of the understory herb Heliconia acuminata \(Heliconiaceae\) in an experimentally fragmented tropical landscape](#). Ecology 104:e4174.
- ³²⁷ Caswell, H. 2001. Matrix population models: Construction, analysis, and interpretation. Sinauer Associates, Sunderland.
- ³²⁹ Cosar, G., and O. Dag. 2024. Vartest: Tests for variance homogeneity. doi: [10.32614/CRAN.package.vartest](https://doi.org/10.32614/CRAN.package.vartest).
- ³³¹ Criley, R., and S. Lekawatana. 1994. [Year around production with high yields may be a possibility for *Heliconia Chartacea*](#). Acta Horticulturae, New ornamental crops and the market for floricultural products 397:95–102.
- ³³⁴ Crone, E. E., E. S. Menges, M. M. Ellis, T. Bell, P. Bierzychudek, J. Ehrlen, T. N. Kaye, et al. 2011. [How do plant ecologists use matrix population models?](#) Ecology Letters 14:1–8.

- ³³⁶ Doak, D. F., W. F. Morris, C. Pfister, B. E. Kendall, and E. M. Bruna. 2005. [Correctly](#)
³³⁷ [Estimating How Environmental Stochasticity Influences Fitness and Population Growth.](#)
- ³³⁸ The American Naturalist 166:E14–E21.
- ³³⁹ Ellner, S. P., D. Z. Childs, and M. Rees. 2016. Data-driven modelling of structured
³⁴⁰ populations: A practical guide to the integral projection model. Springer Science+Business
³⁴¹ Media, New York, NY.
- ³⁴² Ellner, S. P., and M. Rees. 2006. [Integral projection models for species with complex](#)
³⁴³ [demography](#). American Naturalist 167:410–428.
- ³⁴⁴ Evers, S. M., T. M. Knight, D. W. Inouye, T. E. X. Miller, R. Salguero-Gómez, A. M. Iler,
³⁴⁵ and A. Compagnoni. 2021. [Lagged and dormant season climate better predict plant vital](#)
³⁴⁶ [rates than climate during the growing season](#). Global Change Biology 27:1927–1941.
- ³⁴⁷ Kassambara, A. 2023. Rstatix: Pipe-friendly framework for basic statistical tests. doi:
³⁴⁸ [10.32614/CRAN.package.rstatix](https://doi.org/10.32614/CRAN.package.rstatix).
- ³⁴⁹ Kress, J. 1990. [The diversity and distribution of *Heliconia* \(Heliconiaceae\) in Brazil](#). Acta
³⁵⁰ Botanica Brasileira 4:159–167.
- ³⁵¹ Kress, W. J. 1983. [Self-incompatibility systems in Central American *Heliconia*](#). Evolution
³⁵² 37:735–744.
- ³⁵³ Kuss, P., M. Rees, H. H. Ægisdóttir, S. P. Ellner, and J. Stöcklin. 2008. [Evolutionary](#)
³⁵⁴ [demography of long-lived monocarpic perennials: A time-lagged integral projection model](#).
- ³⁵⁵ Journal of Ecology 96:821–832.

- ³⁵⁶ Landau, W. M. 2021. [The targets R package: A dynamic Make-like function-oriented](#)
- ³⁵⁷ [pipeline toolkit for reproducibility and high-performance computing](#). Journal of Open
- ³⁵⁸ Source Software 6:2959.
- ³⁵⁹ Levin, S. C., D. Z. Childs, A. Compagnoni, S. Evers, T. M. Knight, and R.
- ³⁶⁰ Salguero-Gómez. 2021. [Ipmr: Flexible implementation of Integral Projection Models in R](#).
- ³⁶¹ Methods in Ecology and Evolution 12:1826–1834.
- ³⁶² Manly, B. F. 2018. Randomization, bootstrap and Monte Carlo methods in biology.
- ³⁶³ chapman and hall/CRC.
- ³⁶⁴ Metcalf, C. J. E., S. P. Ellner, D. Z. Childs, R. Salguero-Gómez, C. Merow, S. M.
- ³⁶⁵ McMahon, E. Jongejans, et al. 2015. [Statistical modelling of annual variation for inference](#)
- ³⁶⁶ [on stochastic population dynamics using Integral Projection Models](#). Methods in Ecology
- ³⁶⁷ and Evolution 6:1007–1017.
- ³⁶⁸ Molowny-Horas, R., M. L. Suarez, and F. Lloret. 2017. [Changes in the natural dynamics](#)
- ³⁶⁹ [of *Nothofagus Dombeyi* forests: Population modeling with increasing drought frequencies](#).
- ³⁷⁰ Ecosphere 8:1–17.
- ³⁷¹ Morris, W. F., and D. F. Doak. 2002. Quantitative conservation biology: Theory and
- ³⁷² practice of population viability analysis. Sinauer, Sunderland, MA.
- ³⁷³ R Core Team. 2020. *R: A language and environment for statistical computing*. Vienna,
- ³⁷⁴ Austria.
- ³⁷⁵ Rees, M., D. Z. Childs, and S. P. Ellner. 2014. [Building integral projection models: A](#)

- ³⁷⁶ user's guide. Journal of Animal Ecology 83:528–545.
- ³⁷⁷ Rees, M., and S. P. Ellner. 2009. Integral projection models for populations in temporally
³⁷⁸ varying environments. Ecological Monographs 79:575–594.
- ³⁷⁹ ———. 2016. Evolving integral projection models: Evolutionary demography meets
³⁸⁰ eco-evolutionary dynamics. Methods in Ecology and Evolution 7:157–170.
- ³⁸¹ Ribeiro, M. B. N., E. M. Bruna, and W. Mantovani. 2010. Influence of post-clearing
³⁸² treatment on the recovery of herbaceous plant communities in Amazonian secondary
³⁸³ forests. Restoration Ecology 18:50–58.
- ³⁸⁴ Salguero-Gómez, R., O. R. Jones, C. R. Archer, Y. M. Buckley, J. Che-Castaldo, H.
³⁸⁵ Caswell, D. Hodgson, et al. 2015. The COMPADRE Plant Matrix Database: An open
³⁸⁶ online repository for plant demography. (M. Rees, ed.). Journal of Ecology 103:202–218.
- ³⁸⁷ Scott, E. R., M. Uriarte, and E. M. Bruna. 2022. Delayed effects of climate on vital rates
³⁸⁸ lead to demographic divergence in Amazonian forest fragments. Global Change Biology
³⁸⁹ 28:463–479.
- ³⁹⁰ Stouffer, P. C., and R. O. Bierregaard. 1996. Forest fragmentation and seasonal patterns of
³⁹¹ hummingbird abundance in Amazonian Brazil. Ararajuba 4:9–14.
- ³⁹² Tenhumberg, B., E. E. Crone, S. Ramula, and A. J. Tyre. 2018. Time-lagged effects of
³⁹³ weather on plant demography: Drought and *Astragalus Scaphoides*. Ecology 99:915–925.
- ³⁹⁴ Tuljapurkar, S. 1990. Population Dynamics in Variable Environments. (S. Levin, ed.).

- 395 Lecture Notes in Biomathematics (Vol. 85). Springer, Berlin, Heidelberg.
- 396 Tuljapurkar, S., C. C. Horvitz, and J. B. Pascarella. 2003. [The Many Growth Rates and](#)
- 397 [Elasticities of Populations in Random Environments](#). *The American Naturalist*
- 398 162:489–502.
- 399 Uriarte, M., M. Anciães, M. T. B. da Silva, R. Rubim, E. Johnson, and E. M. Bruna. 2011.
- 400 [Disentangling the drivers of reduced long-distance seed dispersal by birds in an](#)
- 401 [experimentally fragmented landscape](#). *Ecology* 92:924–937.
- 402 Williams, J. L., H. Jacquemyn, B. M. Ochocki, R. Brys, T. E. X. Miller, and R. Shefferson.
- 403 2015. [Life history evolution under climate change and its influence on the population](#)
- 404 [dynamics of a long-lived plant](#). *Journal of Ecology* 103:798–808.
- 405 Williams, J. L., T. E. Miller, and S. P. Ellner. 2012. Avoiding unintentional eviction from
- 406 integral projection models. *Ecology* 93:2008–2014.
- 407 Wood, S. N. 2011. [Fast stable restricted maximum likelihood and marginal likelihood](#)
- 408 [estimation of semiparametric generalized linear models](#). *Journal of the Royal Statistical*
- 409 *Society Series B: Statistical Methodology* 73:3–36.
- 410 Xavier, A. C., C. W. King, and B. R. Scanlon. 2016. [Daily gridded meteorological](#)
- 411 [variables in Brazil \(1980–2013\)](#). *International Journal of Climatology* 36:2644–2659.



Description	Deterministic	Stochastic, kernel-resampled	Stochastic, parameter-resampled
Survival	$s(z)$	$s_y(z)$	$s(z; \theta_{0-36})$
Growth	$G(z'; z)$	$G_y(z'; z)$	$G(z'; z; \theta_{0-36})$
Flowering	$p_f(z)$	$p_{f_y}(z)$	$p_f(z; \theta_{0-36})$
Size-specific fecundity	$f(z)$	$f(z)$	$f(z)$
Germination & establishment	g	g	g
Seedling survival	s_0	s_{0_y}	$s_0(\theta_{0-36})$
Seedling growth	$G_0(z')$	$G_{0_y}(z')$	$G_0(z'; \theta_{0-36})$

fig. 1. Life cycle diagram of *Heliconia acuminata*. Each transition is associated with an equation for a vital rate function. The functions shown on the diagram correspond to those used to construct a general, density-independent, deterministic IPM. The table below shows the equivalent equations for stochastic, kernel-resampled IPMs and stochastic, parameter-resampled IPMs.

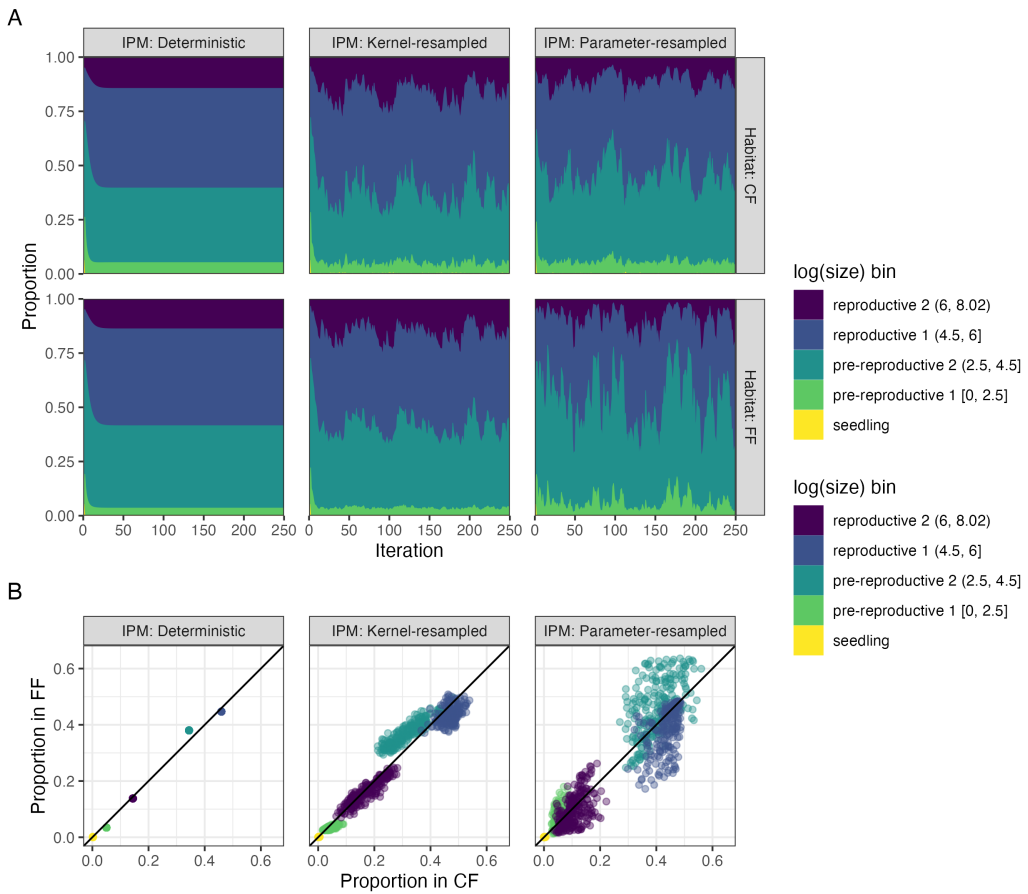


fig. 2. **(A)** The change over time in the the proportion of *Heliconia acuminata* populations in different size/stage classes when simulating population dyammics in Continuous Forest (CF) or Forest Fragment (FF) with three different Integral Projection Models. Results are shown for the first 250 iterations of populations; for the criteria used to define the size categories see Table 3. **(B)** The relative proportion of the population in each size class (FF vs. CF) for 250 iterations of each IPM model. Note that this excludes transient dynamics (iterations 1-30). Values on the 1-1 line indicate an iteration where CF and FF have the same proportion of the population in a given size class.

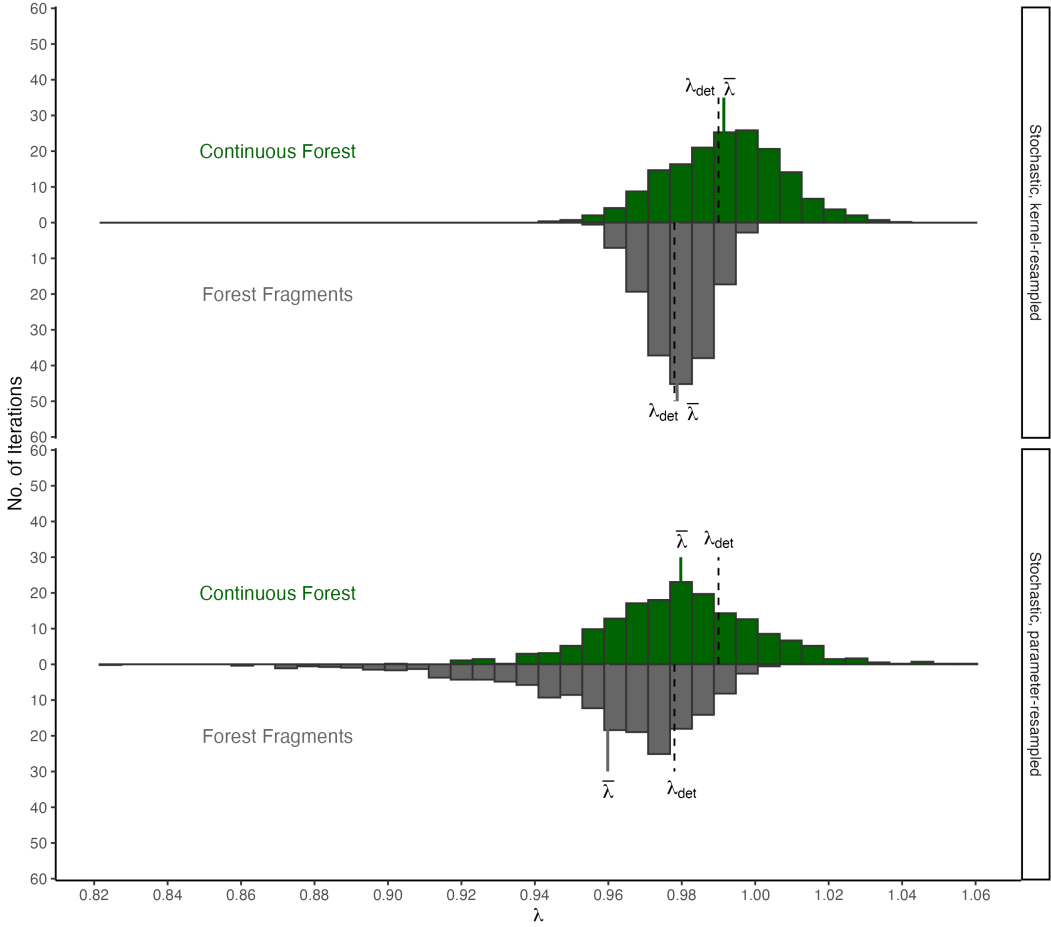


fig. 3. Distribution of 900 values of λ projected with (A) Stochastic, kernel-resampled IPMs and (B) Stochastic, parameter-resampled IPMs. IPMs were used to project λ for both Continuous Forest (above, in green) and Forest Fragments (below, in gray). The solid line indicates the mean value of λ , the dashed line indicates the value of λ in that habitat projected with Deterministic IPMs.

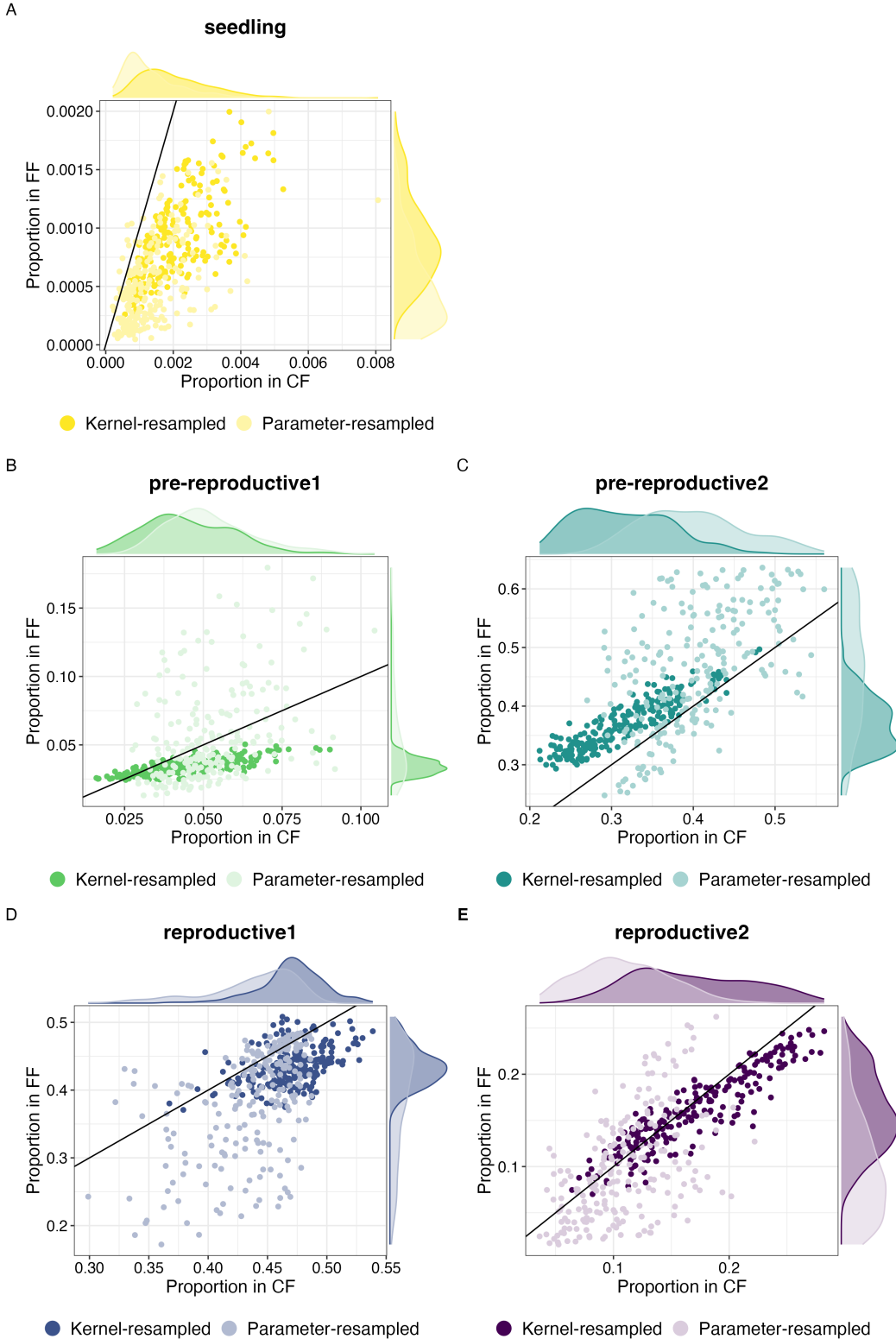


fig. 4. The relative proportion of the population in each size class (FF vs. CF) for each of 250 iterations of the kernel-resampled (dark shading) and parameter-resampled IPM models (light shading). Values on the 1-1 line indicate an iteration where CF and FF have the same proportion of the population in a given size class; the marginal plots indicate the distribution of these relative proportions for each class of IPM in each habitat. Note that both the scatterplots and marginal plots exclude transient dynamics (iterations 1-30).

Table 1: Comparison of vital rate models used to build IPM. The ‘Effect of Environment’ column describes how environmental effects were included in models. Those with ‘none’ were used to build deterministic IPMs; those with a random effect of year were used to build stochastic, kernel-resampled IPMs; and those with a distributed lag non-linear model (DLNM) were used to build stochastic, parameter-resampled IPMs. ‘edf’ is the estimated degrees of freedom of the penalized GAM. ΔAIC is calculated within each habitat and vital rate combination. ΔAIC within 2 indicates models are equivalent.

Habitat	Vital Rate	Effect of Environment	edf	ΔAIC
Continuous Forest				
	Survival	Random effect of year	43.26	0.00
		DLNM	19.72	78.92
		None	4.98	260.01
	Growth	Random effect of year	78.43	0.00
		DLNM	23.87	158.46
		None	7.81	1896.03
	Flowering	DLNM	19.59	0.00
		Random effect of year	17.19	1.63
		None	7.47	381.86
	Seedling survival	None	1.00	0.00
		Random effect of year	1.82	1.39
		DLNM	4.01	1.53
	Seedling growth	Random effect of year	9.47	0.00
		DLNM	8.95	2.90
		None	1.00	172.33
Forest Fragments				
	Survival	DLNM	14.95	0.00
		Random effect of year	19.21	35.68
		None	4.33	51.25
	Growth	DLNM	25.18	0.00
		Random effect of year	37.84	199.98
		None	5.60	382.76
	Flowering	DLNM	20.61	0.00
		Random effect of year	13.81	27.40
		None	5.01	101.70
	Seedling survival	DLNM	5.57	0.00
		Random effect of year	5.09	5.72
		None	1.00	6.49
	Seedling growth	Random effect of year	6.25	0.00
		DLNM	8.18	2.29
		None	1.00	5.74

Table 2: Population growth rates for continuous forest (CF) and forest fragments (FF) under different kinds of IPMs with bootstrapped, bias-corrected, 95% confidence intervals.

IPM	Habitat	λ	(Lower, Upper 95% CI)
Deterministic			
	FF	0.9778	(0.9736, 0.9823)
	CF	0.9897	(0.9877, 0.9920)
Stochastic, kernel resampled			
	FF	0.9787	(0.9735, 0.9835)
	CF	0.9913	(0.9892, 0.9939)
Stochastic, parameter-resampled			
	FF	0.9595	(0.9459, 0.9689)
	CF	0.9795	(0.9752, 0.9867)

Table 3: Size and stage categories used for comparing *Heliconia acuminata* population structure. Note that seedlings are a discrete size class not based on size (see *Methods* for additional details).

Category	Log(size)	Avg. prob. survival	Prob. flowering
Seedlings	-	-	-
Pre-reproductive 1	0–2.5	≤ 0.9	≈ 0
Pre-reproductive 2	2.5–4.5	≥ 0.8	≈ 0
Reproductive 1	4.5–6	≥ 0.95	≤ 0.25
Reproductive 2	≥ 6	≥ 0.95	≥ 0.2

Table 4: Results of statistical tests comparing the variance in the proportion of each habitat's population projected to be in each stage class by kernel-resampled vs. parameter resampled IPMs ($N = 220$ projections per stage class). The variances for each habitat x stage class x IPM combination can be found in Table 5. Comparisons where the p-value of the test was < 0.05 are indicated with an asterisk.

Stage	Habitat	Statistic	df	p value
Seedling				
	CF	4.59	1	0.032*
	FF	11.51	1	0.001*
Pre-reproductive 1				
	CF	8.73	1	0.003*
	FF	96.13	1	< 0.0001*
Pre-reproductive 2				
	CF	0.99	1	0.319
	FF	39.67	1	< 0.0001*
Reproductive 1				
	CF	0.57	1	0.452
	FF	61.58	1	< 0.0001*
Reproductive 2				
	CF	0.11	1	0.745
	FF	18.78	1	< 0.0001*

Table 5: Summary statistics (median, mean, and variance) describing the proportion of populations projected to be in each of five life-history stages by kernel- and parameter-resampled IPMs (N = 220 projections for each IPM class x habitat combination.)

Stage	IPM	Median		Mean		Variance	
		CF	FF	CF	FF	CF	FF
Seedling							
	Kernel-resampled	0.0018	0.0009	0.0020	0.0020	0.000001	0.000000
	Parameter-resampled	0.0011	0.0004	0.0014	0.0014	0.000001	0.000000
Pre-reproductive 1							
	Kernel-resampled	0.0426	0.0340	0.0450	0.0450	0.000203	0.000034
	Parameter-resampled	0.0499	0.0438	0.0522	0.0522	0.000192	0.001167
Pre-reproductive 2							
	Kernel-resampled	0.3097	0.3677	0.3147	0.3147	0.003354	0.001884
	Parameter-resampled	0.3975	0.4613	0.4002	0.4002	0.003934	0.010380
Reproductive 1							
	Kernel-resampled	0.4725	0.4332	0.4704	0.4704	0.000736	0.000822
	Parameter-resampled	0.4464	0.4049	0.4371	0.4371	0.001481	0.006388
Reproductive 2							
	Kernel-resampled	0.1630	0.1554	0.1679	0.1679	0.002630	0.001745
	Parameter-resampled	0.1062	0.0882	0.1092	0.1092	0.001427	0.003213

Table 6: Estimated parameters, standard errors, t-values and P-values for the GLM of the effect of Habitat and IPM Type on projections of lambda.

Term	Estimate	SE	z value	P value
(Intercept)	0.98	0	1568.20	0
$Habitat_{FF}$	-0.02	0	-22.52	0
IPM_{Stoch}	0.01	0	13.27	0
$Habitat_{FF} : IPM_{Stoch}$	0.01	0	5.76	0